EPR study of Ni^+ and Ni^{3+} in x-irradiated CaF_2

J. Casas Gonzalez
Departamento de Física Fundamental, Cátedra de Optica, Universidad de Zaragoza, Zaragoza, Spain

H. W. den Hartog
Solid State Physics Laboratory, 1 Melkweg, Groningen, The Netherlands

R. Alcala
Departamento de Física Fundamental, Cátedra de Optica, Universidad de Zaragoza, Zaragoza, Spain

(Received 7 March 1979)

EPR measurements of CaF_2:Ni crystals before and after room-temperature (RT) x irradiation are reported. Depending on the rare-earth impurity content a small concentration of Ni^+ centers is observed in "as-grown" crystals. During RT x irradiation the Ni^+ concentration increases. At least two different kinds of Ni^+ centers are observed in the EPR spectra. One of them has tetragonal symmetry with $g_{\parallel}=2.569$ and $g_{\perp}=2.089$ and gives a superhyperfine (SHF) structure, due to the interaction with four equivalent fluoride ions, which can be resolved at liquid-nitrogen temperature (LNT). The other one has an almost tetragonal symmetry with g factors and SHF structure very close to the former one but the (SHF) structure is resolved at RT. The first Ni^+ center is associated with a $(NiF_4)^{3-}$ molecular ion with the Ni^+ at a distance of about 0.37 Å from the plane of the fluorine atoms. The other EPR signal is assigned to a similar center with some kind of perturbation. An isotropic EPR signal ($g=2.003$) with a well-resolved superhyperfine structure due to the interaction with eight equivalent fluorines has been detected in some of the samples after RT x irradiation. The tentative model proposed for the center responsible for this signal is a Ni^{3+} ion at a Ca^{2+} substitutional position.

I. INTRODUCTION

Optical and EPR properties of fluorite-type crystals doped with $3d$ ions have been reported[1–6] but the information is less extensive than that concerning rare-earth (RE) impurities, and it is mainly related to as-grown samples. $3d$ ions in CaF_2 are usually incorporated in Ca^{2+} substitutional sites which lead to an unusual cubic environment for these ions. The Jahn-Teller effect which appears in some cases has also been studied both by optical and EPR techniques.[3–6]

Little work has been performed on the radiation effects of these crystals, if we exclude CaF_2:Mn which has received great attention due to its applications in radiation dosimetry. Radiation effects of different ionic crystals doped with $3d$ ions have been studied by several authors.[7–9] Changes in the charge state of the ions as well as the formation of complexes between impurities, and some radiation-induced defects have been observed. In fluorite crystals doped with $3d$ ions several kinds of impurity related defects have been detected after x irradiation. In Co-doped CaF_2, Co^+ ions as well as Co^{2+}-F-center complexes are produced.[10,11] Optical studies of Mn-doped CaF_2 show that Mn^{2+} centers are reduced to Mn^+ by x irradiation at liquid-nitrogen temperature (LNT).[12] In Cu-doped $SrCl_2$, Cu ions enter the lattice as Cu^+ which are converted to Cu^{2+} by x irradiation.[13] Cu^{2+} ions are placed close to the center of one of the faces of the chloride cube forming a kind of $(Cl_4Cu)^{2-}$ molecular ion. Similar results have been obtained in x-irradiated $SrCl_2$:Ag.[14]

In the present paper the EPR spectra of CaF_2:Ni crystals are studied before and after x irradiation. Ni enters CaF_2 as Ni^{2+} in a Ca^{2+} substitutional position[5] but even before irradiation some Ni^+-related centers have been observed. Since rare-earth ions appear as common impurities in CaF_2 the small number of Ni^+ ions observed in "as-grown" crystals can be due to some kind of charge compensation. x irradiation enhances the Ni^+ concentration and creates a number of Ni^{3+} ions. Ni^+ centers show tetragonal symmetry, the ion being placed close to the center of one of the faces of the fluoride cubes giving a kind of $(NiF_4)^{3-}$ molecular complex similar to those reported in Refs. 13 and 14. Ni^{3+} centers have cubic symmetry, the ion being placed in the center of the fluoride cube, showing a strong superhyperfine interaction with the eight fluorines. Optical studies of these centers will be reported in a future paper.

II. EXPERIMENTAL PROCEDURE

The crystals used in the present investigation were prepared by means of the Bridgman technique employing a 25-kW high frequency generator. The crucible material chosen was high purity carbon. The nickel impurities were added to the starting material as NiF_2; the nominal concentrations were about 0.4 mol%. Good crystals which were used were slightly colored (pink).

The irradiation with x rays was carried out with a Philips x-ray generator PW 1008 operating a 40 kV and 17 mA using a Cu target. The bleaching experiments were performed with a 500-W high-pressure mercury lamp, eventually in combination with a Bausch and Lomb monochromator to select the desired wavelength.

The EPR studies were performed using two different frequencies; first, we applied Q-band frequencies (35 GHz) and secondly we employed X-band frequencies (9–10 GHz). Most of the room temperature experiments were carried out under Q-band conditions. For the low-temperature measurements we used the X-band setup.

The experiments at 77 K were performed with an insertion-type liquid-nitrogen cryostat; the crystals were located in the liquid nitrogen. In the setup used, the cryostat had to be refilled once every $\frac{1}{2}$ hour. The variable-temperature experiments were performed using a N_2 flow cryostat.

III. EXPERIMENTAL RESULTS

A. EPR of Ni^+ at RT

In as-grown crystals measured at room temperature (RT) we observed a Q-band EPR signal as shown in Fig. 1. This signal has been taken with $\vec{H} \parallel [100]$. The intensity of this signal, in samples with the same

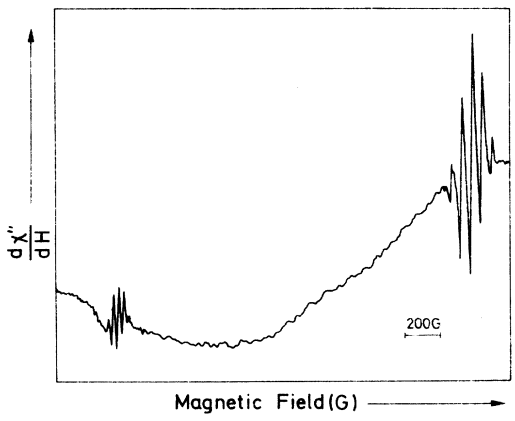

FIG. 1. EPR spectrum of Ni^+ in "as-grown" CaF_2:Ni crystals. Measured at RT under Q-band conditions; $\vec{H} \parallel [100]$.

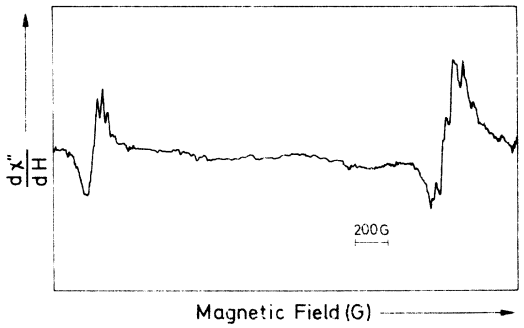

FIG. 2. EPR spectrum of a CaF_2:Ni crystal after x irradiation. Measured at RT under Q-band conditions; $\vec{H} \parallel [100]$.

Ni content, increases with the concentration of RE impurities. The signal shows two resolved patterns which, as it will be discussed later, are associated with Ni^+ centers; the structure of each of these patterns can be explained in terms of superhyperfine interaction between the $3d^9$ electron system and four neighboring ^{19}F nuclei.

In Fig. 2 we show the Q-band EPR signal of a crystal of the same batch as the one from which the spectrum given in Fig. 1 was taken; the only difference being that the sample associated with Fig. 2 has been x irradiated for 15 h at RT. We have found that the intensity of the signals due to Ni^+ has increased (the vertical scale in Figs. 1 and 2 is not the same). Furthermore, it is observed that some unresolved lines have grown at about the same positions as the resolved Ni^+ EPR lines present in as-grown crystals. The ratio of the unresolved and the resolved pattern changes, depending on the purity of the crystals.

When bleaching with white light from a high-pressure mercury lamp, a strong decrease of the EPR signal is observed and the final EPR spectrum consists of resolved patterns only. Similar results can be obtained, when the bleaching is carried out with monochromatic 255-nm light, which corresponds with the absorption band associated with Ni^+ impurities in CaF_2.[15]

B. EPR of Ni^+ at 77 K

The EPR spectrum of an as-grown sample measured at 77 K under X-band conditions is given in Fig. 3. It can be observed that there are two signals due to two different types of Ni^+ centers. The two signals are strongly overlapped in the high-field pattern. The relative intensities of the signals corresponding to these two centers changes from sample to sample.

When the samples are irradiated with x rays at RT and subsequently measured at 77 K we observe that the signal given in Fig. 3 increases and that one of the two patterns becomes dominant. This is shown

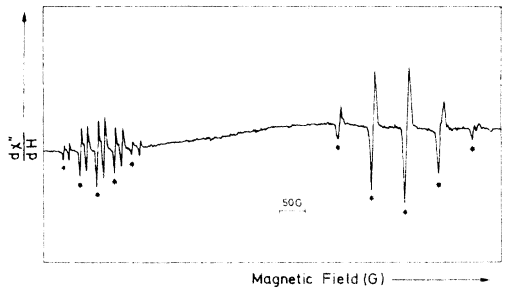

FIG. 3. EPR spectrum of an untreated CaF_3:Ni crystal showing the two types of Ni^+ centers. Measured at LNT under X-band conditions; $\vec{H} \| [100]$.

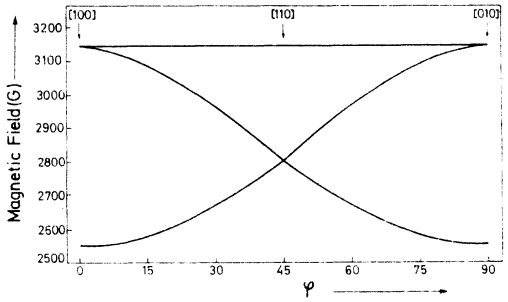

FIG. 5. Rotational diagram corresponding to the central lines of the marked spectrum given in Fig. 3. Measured at LNT under X-band conditions.

in Fig. 4(a) in which we have only given the low-field signal. The dominant pattern is marked with a star. Optical bleaching either with white light or with 255-nm light produces a decrease of the signal. The dominant pattern is affected more strongly [Fig. 4(b)]. [The vertical scale for Figs. 4(a) and 4(b) is different. The intensity in Fig. 4(b) being much smaller than that in Fig. 4(a).]

In order to study the symmetry of the centers under consideration we have produced rotational diagrams of the EPR patterns. In Fig. 5 we show the rotational diagram which corresponds to the marked spectrum in Fig. 3 during rotation in the (100) plane. We have only plotted the positions of the central EPR lines. From Fig. 5 we see that the center has tetragonal symmetry. We will see later that the ground level of the Ni^+ center can be thought of as an effective $S = \frac{1}{2}$ state. The pattern at high field (see Fig. 3) is due to Ni^+ centers having the C_4 axis perpendicular to the magnetic field. For $\vec{H} \| [100]$ the low-field pattern is associated with centers having the C_4 axis parallel to H. From the structure of the superhyperfine patterns we have obtained information about the interaction between the paramagnetic electron system and the magnetic ^{19}F nuclei. The magnetic parameters as given in the spin Hamiltonian Eq. (1), have been compiled in Table I. The x,y,z axes are along the $\langle 100 \rangle$ crystallographic directions. The z' axis for each ligand is along the Ni $-$F line, (see Fig. 8)

$$H = \mu_B [g_{\parallel} H_z S_z + g_{\perp}(S_x H_x + S_y H_y)] + \sum_{i=1}^{4} [(S_x' I_x'^i + S_y' I_y'^i) A_{\parallel} + S_z' I_z'^i A_{\perp}] \quad . \qquad (1)$$

The rotational diagram of the unmarked pattern in Fig. 4 is similar to that of the marked one; however, small but significant differences have been observed, showing that the symmetry of the Ni^+ centers associated with the unmarked lines is lower than tetragonal. We associate this departure from the tetragonal symmetry to the presence of some other defect (probably a RE impurity) that perturbs the pure Ni^+ center.

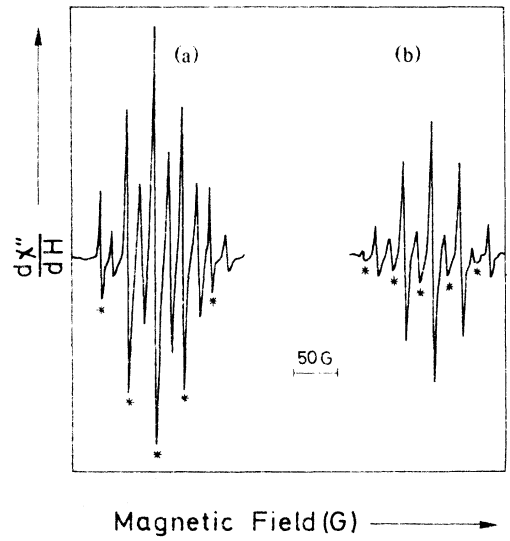

FIG. 4. Change in the population ratio obtained by RT bleaching with 255-nm light. (a) Before bleaching. (b) After bleaching. Only the parallel spectrum is shown. Measured at LNT under X-band conditions; $\vec{H} \| [100]$.

TABLE I. EPR parameters for the unperturbed Ni^+ center in CaF_2 measured at 77 K.

$g_{\parallel}$	$g_{\perp}$	$A_{\parallel}$ (10^{-4} cm^{-1})	$A_{\perp}$ (10^{-4} cm^{-1})
2.569 ± 0.005	2.089 ± 0.005	81.3 ± 3	36.5 ± 3

C. Temperature dependence

In order to understand the difference between low-temperature and RT spectra we have measured the signal at different temperatures in the range 77–300 K.

In Fig. 6 we give the patterns corresponding to parallel centers for $\vec{H} \parallel [100]$ taken at 213, 233, and 258 K. It can be seen that only the marked lines strongly broaden as a function of temperature.

This explains the broad signals found at RT. On the other hand, since the optical bleaching destroys preferentially the pattern that broadens with T, we can also account for the bleaching behavior observed in the RT spectra.

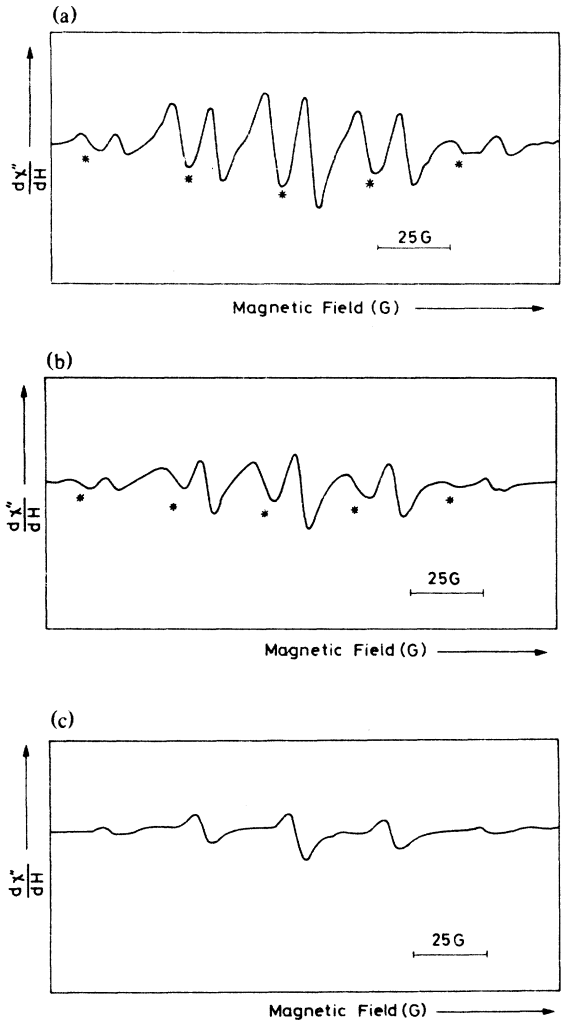

FIG. 6. Thermal evolution of the EPR spectrum. (a) Measured at 213 K, (b) at 233 K, (c) at 258 K. (The parallel transition is shown. X-band conditions; $\vec{H} \parallel [100]$.)

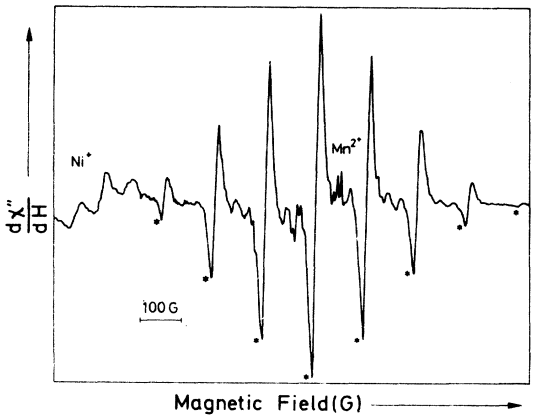

FIG. 7. Marked lines correspond to the cubic signal seen in RT x-irradiated samples. The lowest field peak of the multiplet is masked by a signal due to Ni^{+}. A weak signal due to small amounts of Mn^{2+} is also present. Measured at RT under Q-band conditions; $\vec{H} \parallel [100]$.

D. Cubic signal

After RT x irradiation we find, in some of the crystals a signal showing cubic symmetry properties. This signal has been observed only at RT under Q-band conditions. The most interesting features of this signal are the isotropic g factor ($g = 2.003$) and the large superhyperfine splitting. The signal observed for $\vec{H} \parallel [100]$ has been given in Fig. 7; it shows nine equidistant lines with an intensity ratio of approximately 1:8:28:56:70:56:28:8:1. This signal has been tentatively associated to a Ni^{3+} ion in a Ca^{2+} substitutional position. As it will be discussed later the ground level of this Ni^{3+} center can be thought of as an effective $S = \frac{3}{2}$ state in which the superhyperfine structure corresponding to transitions between the $M_S = -\frac{3}{2} \leftrightarrow -\frac{1}{2}$, $-\frac{1}{2} \leftrightarrow \frac{1}{2}$, $\frac{1}{2} \leftrightarrow \frac{3}{2}$ Zeeman levels coincides. The structure can be explained as due to the interaction of the electron system with eight equivalent ^{19}F nuclei. The magnetic parameters as given by the spin Hamiltonian Eq. (2) have been compiled in Table II. The z axis is along the $\langle 111 \rangle$ crystallographic directions

$$H = g\mu_B \vec{H} \cdot \vec{S} + \sum_{i=1}^{8} [(S_x I_x^i + S_y I_y^i) A_{\parallel} + S_z I_z^i A_{\perp}] \ .$$

TABLE II. EPR parameters for the cubic signal in CaF_2 measured at RT under Q-band conditions.

g	$A_{\parallel}(10^{-4}\ cm^{-1})$	$A_{\perp}(10^{-4}\ cm^{-1})$
2.003	181.6 ± 3	64.7 ± 3

IV. DISCUSSION

Optical-absorption experiments in RT x-irradiated CaF_2:Ni indicate that an absorption band that appears at 255 nm is associated with Ni^+ centers oriented along the ⟨100⟩ directions of the lattice.[15] The 255-nm band is created by x irradiation, and destroyed by optical bleaching with 255-nm light. The experiments reported in Fig. 4 show that the EPR signal presents the same behavior under x irradiation and subsequent optical bleaching. On the other hand the rotational diagrams indicate that the center responsible for the EPR signal has C_{4v} symmetry with the C_4 axis along the ⟨100⟩ directions. From all this we conclude that the 255-nm band and the EPR signal are due to the same center that has been proposed[15] to be associated with a Ni^+ ion.

There are several ways to explain the tetragonal symmetry of the center: (i) there is a Jahn-Teller distortion, (ii) there is an extra point defect in the neighborhood of the Ni^+ center, (iii) there is a displacement of the Ni^+ impurity away from the substitutional Ca^{2+} site.

In our opinion the fact that we have observed appreciable superhyperfine interaction with only four out of eight neighboring fluorine nuclei excludes the Jahn-Teller effect as a possible origin of the tetragonal distortion.

The most likely extra defect that could produce a reduction of cubic to tetragonal symmetry is the interstitial fluoride ion. In this case one obtains centers which are similar to the charge compensation complexes observed in CaF_2 crystals doped with trivalent rare-earth ions.[16] We note, however, that the effective charge of the Ni^+ center is $-e$ and this charge will repel the eventual interstitial F^- ions in the vicinity. Also in crystals doped with NiF_2 there will be only very few interstitial F^- ions present as charge compensation is not necessary, and since the Ni^+ signal increases during x irradiation we would need to create fluorine interstitials but there is no evidence for the formation of the complementary vacancy centers. Some of these objections also apply if the extra defect giving tetragonal symmetry is a neutral interstitial fluorine. On the other hand this fluorine atom would likely form a kind of H_A center that would not give the tetragonal symmetry. Furthermore no EPR signal corresponding to the interstitial atom has been observed.

The possibility of a displacement of the Ni^+ ion away from the Ca^{2+} site remains. Similar centers have been reported by Moreno[14] on the system $SrCl_2$:Ag^{2+} and Bill[13] on the system $SrCl_2$:Cu^{2+}. For these two systems the authors conclude that the impurity is located approximately in the plane of four lattice Cl^- ions. In a similar way we propose for our tetragonal center the model given in Fig. 8. The value of $\alpha = 11°$ has been obtained by fitting our data to the spin Hamiltonian Eq. (1). According to our results the Ni^+ ion is located about 0.37 Å out of the plane of the four fluoride ions but this value should be corrected for relaxation effects of the fluoride ion involved.

The model for the Ni^+ center with symmetry lower than tetragonal is basically the same as the one given in Fig. 8. No particular model is proposed for the perturbation causing the departure from tetragonal symmetry.

We assume that the nickel impurity and the four lattice fluoride ions form an almost planar complex with strongly covalent bonds. This leads to a mixing of the Ni^+ wave functions and those of the F^- ions and consequently the hyperfine interaction between the Ni^+ $3d^9$ electron system and the ^{19}F nuclei of the complex is relatively large. Thus the center is in fact a $(NiF_4)^{3-}$ molecular ion in the CaF_2 crystal and the observations should be comparable with those of other planar complexes, e.g., cupric phthalocyanine and silver phthalocyanine, where one is dealing with the $3d^9$ electron configurations of Cu^{2+} and Ag^{2+}, respectively.[17]

From molecular orbital theory an energy diagram has been given for square planar complexes containing an ion with a $3d^9$ electron configuration.[17] In addition, also, a probable splitting pattern has been given for square pyramidal complexes. This pattern has been reproduced in Fig. 9. The energy levels shown in Fig. 9 have to be filled with nine electrons and it can be seen that there is an unpaired electron in the d_{xy} orbit. So the ground state of the Ni^+ ion would have an effective spin $S = \frac{1}{2}$. We note that as a result of a rotation of the frame of axes, the states $d_{x^2-y^2}$ and d_{xy} have been interchanged with respect to those given in Ref. 17.

With our experimental results the term scheme as given in Fig. 9 can be checked to some extent. For

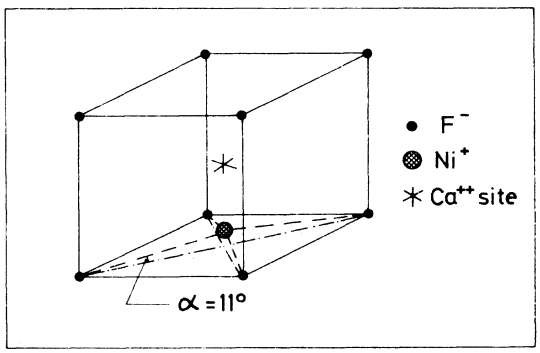

FIG. 8. Proposed model for the Ni^+ defect in CaF_2:Ni.

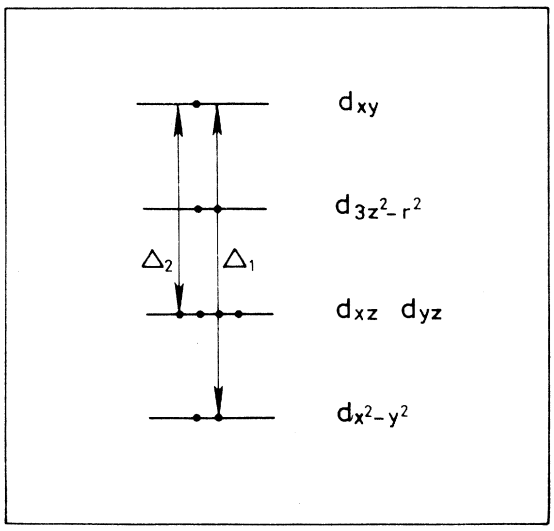

FIG. 9. Energy-level diagram for the $(NiF_4)^{3-}$ complex.

the electronic g factors we can write the following relations[18]

$$g_{\parallel}=2-\frac{8\lambda}{\Delta_1}-3\left(\frac{\lambda}{\Delta_2}\right)^2-\frac{4\lambda^2}{\Delta_1\Delta_2}\ , \tag{3a}$$

$$g_{\perp}=2-\frac{2\lambda}{\Delta_2}-4\left(\frac{\lambda}{\Delta_1}\right)^2\ . \tag{3b}$$

From the experimental values obtained for $g_{\parallel}$ and $g_{\perp}$, taking for λ a value of $-450\ cm^{-1}$ we find[19] $\Delta_1=4900\ cm^{-1}$ and $\Delta_2=8000\ cm^{-1}$. Comparing this result with the level scheme shown in Fig. 9, we conclude that the energy level associated with d_{xz}, d_{yz} is lower than the $d_{x^2-y^2}$ level. We feel that this result is not in contradiction with the theoretical description given by Figgis[17] because the diagram in Fig. 9 has only been presented as a probable level diagram. We also note that the position of the $d_{3z^2-r^2}$ cannot be checked with the present experimental results; the only conclusion about this level can be that it is not the highest level, because the g factors would be very much different from the ones we have observed (see also Hayes and Wilkens[19]).

The conclusion that the unpaired electron is in a d_{xy} orbit is in agreement with the strong interaction between this electron and four F nuclei surrounding the Ni^+ ion. This picture enables us to understand also the fact that the hyperfine interaction with the other four F nuclei surrounding the Ni^+ impurity is not observable. The overlap between the Ni^+ d_{xy} orbit and the other F^- electron cores is very small.

With respect to the formation of Ni^+ centers we can say the following. The small concentration of Ni^+ before any treatment can be due to charge compensation for trivalent RE impurities. The bigger number of Ni^+ centers observed when RE concentration increases seems to be in favor of this explanation.

During x irradiation the concentrations of the Ni^+ centers are enhanced. It is well known that during x irradiation electrons and holes are created in the CaF_2 lattice.[16] Stable defects can be formed only if both the hole and the electron are trapped somewhere in the lattice. We know that at room temperature a self-trapped hole (V_k center) is not stable and will recombine easily with electron centers. Impurities may stabilize the holes and may therefore increase the formation rate of Ni^+ centers.

In a CaF_2:Ni^{2+} crystal in which there are no other impurities than Ni^{2+} it will be necessary to form Ni^{3+} in order to produce Ni^+ centers. It is interesting to note that the cubic signal that we tentatively assign to Ni^{3+} centers has only been observed in crystals where no other impurities were present. That is one of the reasons to associate the cubic signal to Ni^{3+}.

On the other hand trivalent Ni impurities have a $3d^7$ electron configuration. In eightfold cubic coordination the ground state is a $^4A_{1g}$ (Ref. 1) that can be thought of as an effective $S=\frac{3}{2}$ state. There is no zero-field splitting of this level in cubic symmetry. Since the g factor is very close to the free-electron value we expect[20] that additional third-order terms in the spin Hamiltonian Eq. (2) will be very small. With the energy levels given by Eq. (2) only one set of superhyperfine lines is expected with an intensity ratio 1:8:28:56:70:56:28:8:1 in agreement with the experimental results.

The very small g shift and the high superhyperfine interaction of this Ni^{3+} center as compared with other $3d^7$ ions in tetrahedral and eightfold coordination[21,22,23] are remarkable. A tentative explanation for these facts can be given by assuming a very strong crystal field due to the relaxation of the eight fluoride ions toward the Ni^{3+} which has an effective positive charge. The strong crystal field (and also some covalency) would produce a decrease of the g factor and an increase of the superhyperfine interaction.

Another significant difference between Ni^{3+} and other $3d^7$ ions is the long relaxation time (the signal is observed at RT). We do not have any clear explanation for this fact. Clearly more work has to be done on this center in order to draw sound conclusions.

ACKNOWLEDGMENTS

The authors wish to thank P. Wesseling for growing the crystals. Two of us (J.C.G. and R.A.) are indebted to the CSIC and to the IEN (Spain) for financial support.

[1]R. Stahl-Brada and W. Low, Phys. Rev. 113, 775 (1959).
[2]E. I. Zoroarskaya, B. Z. Malkin, A. L. Stolov, and Zh. S. Yakovleva, Sov. Phys. Solid State 10, 255 (1968).
[3]W. Ulrici, Phys. Status Solidi B 62, 431 (1974).
[4]P. J. Alonso and R. Alcalá, Phys. Status Solidi B 81, 333 (1977).
[5]M. M. Zaripov, V. S. Kropotov, L. D. Livanova, and V. G. Stepanov, Sov. Phys. Solid State 9, 155 (1967); 9, 2344, 2346, 2347 (1968); 10, 262 (1968).
[6]U. T. Höchli, Phys. Rev. 162, 262 (1967).
[7]S. I. Yun, L. A. Kappers, and W. A. Sibley, Phys. Rev. B 8, 773 (1973).
[8]K. H. Lee and W. A. Sibley, Phys. Rev. B 12, 3392 (1975).
[9]M. Ikeya and N. Itoh, J. Phys. Soc. Jpn. 29, 1295 (1970).
[10]R. Alcalá and P. J. Alonso, Phys. Rev. B 18, 5506 (1978).
[11]R. Alcalá and P. J. Alonso, J. Lumin. 20, 1 (1979).
[12]P. J. Alonso and R. Alcalá, J. Lumin. (in press).
[13]H. Bill, Phys. Lett. A 44, 101 (1973).
[14]M. Moreno, Ann. Fis. 70, 261 (1974).
[15]J. Casas, H. W. den Hartog, and R. Alcalá, Proceedings International Conference on Point Defects in Ionic Crystals, Canterbury, England, 1979 (unpublished).
[16]*Crystals With the Fluorite Structure*, edited by W. Hayes (Clarendon, Oxford, 1974), Chaps. 5, 6, 7.
[17]B. N. Figgis, *Introduction to Ligand Fields* (Wiley-Interscience, New York, 1966), p. 320.
[18]B. Bleaney, K. D. Bowers, and M. H. L. Pryce, Proc. R. Soc. London Ser. A 228, 166 (1955).
[19]W. Hayes and J. Wilkens, Proc. R. Soc. London Ser. A 281, 340 (1964).
[20]F. S. Ham, G. W. Ludwig, G. D. Watkins, and H. H. Woodbury, Phys. Rev. Lett. 5, 468 (1960).
[21]T. P. P. Hall and W. Hayes, J. Chem. Phys. 32, 1871 (1960).
[22]R. K. Watts, Phys. Rev. 188, 568 (1969).
[23]K. E. Roelfsema and H. W. den Hartog, J. Magn. Reson. 29, 255 (1978).